Atom Indonesia

Journal homepage: http://aij.batan.go.id

Structure and Decay Properties of Th Isotopes Using E-RMFT Formalism

M. Das, K. C. Naik, N. Biswal, R. N. Panda*

[1]*Department of Physics, Siksha 'O' Anusandhan Deemed to be University, Bhubaneswar-751 030, India*

ARTICLE INFO

Article history:
Received 20 June 2021
Received in revised form 25 May 2022
Accepted 2 June 2022

Keywords:
Binding energy
Neutron-skin
Excitation energy
Specific heat
Decay energy
Decay half-life

ABSTRACT

In the present scenario, the search for the thermally fissile nuclei is crucial and also important not only for the research background of nuclear physics but also for the great social and economic impact on the country. Many theoretical works have been performed to analyze a series of Th and U-isotopes and found that some of these isotopes are stable against α-decays and spontaneous fission. Here, we have chosen the isotopic chain of Th-nuclei for the present analysis using relativistic mean-field formalism. The work also explores a few stable isotopes in this region of the nuclear landscape, which is crucial for understanding the exotic region of the nuclear landscape. The objective of this work is to study the bulk properties such as binding energies, root mean square charge radii, neutron-proton radii, neutron skin-thickness as well as intrinsic properties such as excitation energy and specific heat for the $^{216-238}$Th-isotopic chain. Furthermore, the stability of these isotopes is investigated through their possible decay chain analysis. The relativistic mean-field theory was used to obtain the nuclear bulk properties, namely, binding energies, root-mean-square charge radii, neutron skin-thickness, and excitation energy. The steady solution of the temperature-dependent effective relativistic mean-field equations was obtained self-consistently by taking different inputs of the initial deformations. All the calculations were done for NL3, FSUGarnet and IOPB-I parameter sets for $^{216-238}$Th-isotopes. The decay energy of α (Q_α) and β-decay (Q_β) were calculated from the binding energies and were further used to obtain the corresponding half-lives. We have analyzed the structural and decay properties of $^{216-238}$Th isotopes. The excitation energy and specific heat are also estimated for these considered nuclei by using the temperature-dependent effective relativistic mean-field (E-RMFT) formalism for NL3, FSUGarnet and IOPB-I parameters sets. The calculated results are compared with the available experimental data and found similar observations for all the parameter sets at a given temperature. The excitation energy study signifies the shell melting point where maybe the shape transition occurs. Three phenomenological formulae such as Viola-Seaborg, Royer and modified universal decay law are adopted for the calculation of α-decay half-lives. We found lower values of α-decay half-lives indicating a higher rate of β-decay for the isotopic chain.

INTRODUCTION

Presently, ~3000 nuclei are known to us and another 5000 nuclei with varying lifetimes have been predicted and can be synthesized experimentally [1,2]. Almost all of these isotopes are found on the neutron-rich edge of the nuclear chart and possess unusual neutron to proton proportion. Since 1940, after the discovery of fission phenomena, there has been tremendous progress to study the fission dynamics of the above exotic nuclei. Out of the 300 nuclei, nature gave us three options for fissile fuels (^{233,235}U, and ^{239}Pu), which are thermally fissile on the stability line and are used for the power generation in reactors [3,4].

Satpathy collaborators [5] in the year 2008, suggested and mentioned that the series of Th and U isotopes with neutron numbers ranging from 154-172 to be thermally fissile. They found these results by calculating the fission barrier and neutron separation energy [6]. Their results show that some

*Corresponding author.
E-mail address: rnpandaphy@gmail.com
DOI: https://doi.org/10.17146/aij.2022.1156

isotopes in that series are stable against α-decay as well as spontaneous fission [7]. In addition to these, the shell correction energy, deformation parameters, the asymmetry energy coefficient etc., are also crucial quantities to study the structure and dynamics of a nucleus [5,8-14].

The alpha-decay process is one of the basic topics in theoretical and experimental nuclear physics. This phenomenon has a vital role in the success of different nuclear models, as it provides various information on the nuclear properties of nuclei [15]. The stability of nuclei can be attained by making a balance between the attractive nuclear force and the repulsive Coulomb force [16]. Furthermore, the disclosure of α-decay by Becquerel in 1986 and its theory by Gammow et. al in 1928, is a front-line nuclear property, which is used for the structural analysis of neutron-rich isotopes. Basically α-decay is a two-decay mode which starts from α-decay and ends with spontaneous fission.

Kumar et al [17] surveyed the various decay chains for Th and U-isotopes within the framework of relativistic mean-field (RMF) theory. They have shown that these two isotopes are stable against α and cluster decays. In addition to this, these nuclei are highly β-unstable and also the lifetime for β-decay is higher in comparison to α-decay. In the above cases, spontaneous fission does not take place due to the neutron-richness of nuclei which broadens the fission barrier.

Currently, the microscopic relativistic mean-field approximation is also used to analyze nuclear fission and also for other modes of decay. Extrapolation of neutron-rich (having more neutron numbers), super-heavy isotopes plays a crucial role due to their ground state structures, different modes of decay and multi-fragment fission [12]. Besides their thermally fissile nature, these nuclei also have a major part in the nucleosynthesis in stellar evolution.

Previously, the half-life of the α-decay for Th-isotopes has been calculated using WKB Semi-classical approximation taking the help of the Bohr-Sommerfield quantization condition. The relativistic mean-field theory can be employed for both density-dependent and independent M3Y, R3Y-interactions to calculate α-decay half-lives [18]. Many experimental laboratory facilities like Dubna (Russia), GSI (Germany), RIKEN (Japan), and BNL (USA) extended the number of elements (known to be neutron-rich or super-heavy nuclei) in the periodic table up to Z = 118 as well as they can synthesize the newly formed nuclei [19]. After this, it becomes quite easy to study their ground state properties, decay chain, nuclear asymmetry energy and many more. The experimental observations of Z≤118 showed that there is a probability of the existence of neutron-excess isotopes with the increase of atomic number. This signifies the enhancement shell effects with the rise of Z-values [20].

In the present work, we aim to investigate the bulk properties like binding energies (BE), root-mean-square charge radii (R_{ch}), neutron-skin thickness (ΔR) and intrinsic properties like excitation energy and specific heat of $^{216-238}$Th nuclei with recently developed force parameters (FSUGarnet, IOPB-I) [21,22]. As an important task, we have also studied α-decay half-lives using three phenomenological formulae such as Viola-Seaborg, Royer's empirical formula and modified universal decay law using the decay energy Q_α values. Finally, we pay attention to check the β-stability through β-decay half-lives. The paper is structured as follows: In section II, the E-RMFT formalism is discussed briefly. Here, we represent the equation of motion for the nucleon as well as meson fields. In Section III, the observed values are given in detail. Lastly, in Section IV, the summary and concluding remarks of our work are analyzed.

THEORETICAL FORMALISM

E-RMFT theory

To calculate the important bulk properties of a nucleus like binding energy, charge radius, neutron skin-thickness etc., many theoretical models can be found. Out of these, the most successful relativistic mean theory is a relativistic conception of non-relativistic theory and it has the extra benefit to work better in the high-density range. Another importance of this model is that the spin-orbit interaction for finite nuclei is also taken care of automatically. In this extensive study, we explain the E-RMFT formalism briefly [23]. The fundamental nucleon-meson Lagrangian density in the framework of E-RMFT up to 4th order with mesons and photons is written as [21,22] in Eqs. (1-4).

$$\mathcal{L}(r_\perp, z) = \bar{\Phi}(r_\perp, z)(i\gamma^\mu\partial_\mu - M + g_s\sigma - g_\omega\gamma^\mu\omega_\mu)\Phi(r_\perp, z) + \frac{1}{2}(\partial^\mu\sigma\partial_\mu\sigma - m_s^2\sigma^2) - \frac{1}{4}V^{\mu\nu}V_{\mu\nu} + \frac{1}{2}m_\omega^2\omega^\mu\omega_\mu - \frac{1}{4}\vec{R}^{\mu\nu}\vec{R}_{\mu\nu} + \frac{1}{2}m_\rho^2\vec{\rho}^\mu\vec{\rho}_\mu - \frac{1}{4}F^{\mu\nu}F_{\mu\nu} - \Lambda_\omega g_\omega^2 g_\rho^2(\omega^\mu\omega_\mu)(\vec{\rho}^\mu\vec{\rho}_\mu), \quad (1)$$

with

$$V^{\mu\nu} = \partial^\mu\omega^\nu - \partial^\nu\omega^\mu \quad (2)$$

$$\vec{R}^{\mu\nu} = \partial^\mu\vec{\rho}^\nu - \partial^\nu\vec{\rho}^\mu \quad (3)$$

$$F^{\mu\nu} = \partial^\mu A^\nu - \partial^\nu A^\mu \quad (4)$$

where σ, ω and ρ are the meson fields along with the coupling constants g_s, g_ω, g_ρ and masses m_σ, m_ω and m_ρ respectively. The A_μ, which provides electromagnetic interaction is the photon field, with coupling strength $e^2/4\pi$. By defining fields as $\Phi = g_s\sigma$, $W = g_\omega\omega^0$, $R = g_\rho\vec{\rho}^0$ and $A = eA^0$, the Dirac equation in the axially deformed coordinates is written as [23] in Eq. (5).

$$\{-i\alpha.\nabla + \beta\,[M - \phi(r_\perp, z)] + W(r_\perp, z) + \frac{1}{2}\tau_3 R(r_\perp, z) + \frac{1+\tau_3}{2} A(r_\perp, z)\}\phi_\alpha(r_\perp, z) = \varepsilon_\alpha \varphi_\alpha(r_\perp, z) \quad (5)$$

The mean-field equations for ϕ, W, R and A are given by Eqs. (6-9).

$$-\Delta\phi(r_\perp, z) + m_s^2\phi(r_\perp, z) = g_s^2\rho_s\phi(r_\perp, z) - \frac{m_s^2}{M}\phi^2\phi(r_\perp, z)\left(\frac{\kappa_3}{2} + \frac{\kappa_4}{3!}\frac{\phi(r_\perp, z)}{M}\right) \quad (6)$$

$$-\Delta W(r_\perp, z) + m_\omega^2 W(r_\perp, z) = g_\omega^2\rho(r_\perp, z) - \frac{1}{3!}\zeta_0 W^3(r_\perp, z) - 2\Lambda_\omega R^2(r_\perp, z)W(r_\perp, z), \quad (7)$$

$$-\Delta R(r_\perp, z) + m_\rho^2 R(r_\perp, z) = \frac{1}{2}g_\rho^2\rho_3(r_\perp, z) - 2\Lambda_\omega R(r_\perp, z)\, W^2(r_\perp, z) \quad (8)$$

$$-\Delta A(r_\perp, z) = e^2\rho_p(r_\perp, z) \quad (9)$$

RESULTS AND DISCUSSION

We have aimed to investigate some of the fundamental properties like binding energies, rms charge radii, and neutron-skin thickness of even-even $^{216-238}$Th nuclei at finite temperature. The relativistic temperature-dependent i. e E-RMFT method is used by taking the currently established force parameters i.e FSUGarnet and IOPB-I. Also, it is compared with the results of the most successful NL3 parameter set as well as with the available experimental data. These results are depicted in Table 1. Then, we studied the intrinsic quantities like nuclear excitation energy and specific heat with the application of temperature. In addition to this, to examine the stability of nuclei, the decay studies of Th-isotopes are included.

The α-decay energy (Q_α) and half-lives are calculated using three different formulae and the β-decay energy (Q_β) and corresponding half-lives are also evaluated using the empirical formula for NL3, IOPB-I parameters and compared with experimental data. In Tables 1 and 2 and Figs. 1-3, we have represented all the calculated results. At first, the motivation for choosing parameters is introduced, and then we have analyzed the results of our calculations.

Parameters

Nearly 265 parameter sets are exist in the literatures [22,24,25] to explain the properties of the nucleus. In RMF**,** every term has its significance. In the Walecka-model, mesons have no interaction between themselves. As a result, the incompressibility K_∞ is very high i. e. ≈ 550 MeV (experimental limits 210±30 MeV) [26]. Then Boguta and Bodmer [27-29] introduced self-coupling terms in σ meson which decreases the value of K_∞ to 211 MeV at saturation of infinite nuclear matter [30]. Again, it was unable to reproduce the nuclear equation of states (EoS) up to satisfaction. So, there is a need for a non-linear term which is important to soften the nuclear EoS [31]. Later on, Todd-Rutel and Piekarewicz [32-34] introduced the cross-coupling terms of ρ- and ω-mesons in the original formalism of Furnstahl *et al*. [23] to take care of the radius of neutron stars well as neutron-skin thickness, whereas the self-coupling of ω-meson ζ_0 is used to tune the limiting mass of neutron star [25]. In this work, three force parameters namely NL3 [35], FSUGarnet [21] and IOPB-I [22] are used to calculate the nuclear observable. We find the results obtained from the above three parameter sets are in harmony with each other which implies that one can rely on these forces.

Binding energy

The amount of energy required to ascertain the nuclei together is called the binding energy. Our calculated results for the bulk property binding energy (BE) at zero temperature for nuclei $^{216-238}$Th using different parameters such as NL3, FSUGarnet, and IOPB-I are tabulated in Table 1. The obtained values are also compared with the available experimental data [19,36]. It is clear from Table 1 that our results for the above parameter sets are comparable to the data. Here the calculated results are found to be in agreement with the available data for all the considered force parameters. For example, the experimental binding energy of ^{226}Th = 1734.28 MeV and the RMF result with G3 is 1730.51 MeV, which has an accuracy of more than 99 %. A detailed observation of Table 1 gives BE as predicted in NL3 slightly overestimates the FSUGarnet and IOPB-I results.

The BE values for all the three parameters as well as the data increases with the mass number. The BE/A analysis suggests that maximum value can be seen for ^{226}Th-isotope for all the parameter sets, signifying that it is the most stable isotope among this considered isotopic chain. Generally, results calculated from the above three parameter sets are acceptable, and one can use these forces for further predictions even at finite temperatures.

Table 1. Different bulk properties like the ground state binding energy (MeV), charge radius R_{ch} (fm) and neutron skin thickness ΔR (fm) for $^{216-238}$Th corresponding to NL3 [35], FSUGarnet [21] and IOPB-I [22] sets and available experimental data (EXP.) [36,37].

Nucl.	Obs.	NL3	FSUGarnet	IOPB-I	EXP.
	BE	-1672.19	-1667.27	-1668.87	-1662.69
^{216}Th	**R_{ch}**	5.648	5.627	5.663	
	ΔR	0.183	0.093	0.136	
	BE	-1685.77	-1679.26	-1680.18	-1676.77
^{218}Th	**R_{ch}**	5.661	5.643	5.682	
	ΔR	0.191	0.099	0.143	
	BE	-1698.71	-1690.93	-1692.80	-1690.61
^{220}Th	**R_{ch}**	5.688	5.667	5.704	
	ΔR	0.201	0.105	0.152	
	BE	-1711.17	-1703.37	-1705.29	-1704.22
^{222}Th	**R_{ch}**	5.709	5.687	5.725	
	ΔR	0.210	0.111	0.160	
	BE	-1722.60	-1715.29	-1717.25	-1717.57
^{224}Th	**R_{ch}**	5.729	5.705	5.745	
	ΔR	0.219	0.117	0.167	
	BE	-1734.28	-1726.47	-1728.49	-1730.51
^{226}Th	**R_{ch}**	5.749	5.724	5.764	
	ΔR	0.226	0.122	0.174	
	BE	-1745.51	-1735.23	-1737.52	-1743.08
^{228}Th	**R_{ch}**	5.767	5.737	5.776	5.749
	ΔR	0.234	0.137	0.192	
	BE	-1756.33	-1744.44	-1746.82	-1755.13
^{230}Th	**R_{ch}**	5.778	5.753	5.793	5.767
	ΔR	0.254	0.141	0.197	
	BE	-1767.55	-1753.05	-1755.73	-1766.69
^{232}Th	**R_{ch}**	5.789	5.765	5.805	5.785
	ΔR	0.273	0.155	0.214	
	BE	-1777.65	-1761.48	-1764.45	-1777.66
^{234}Th	**R_{ch}**	5.800	5.777	5.815	
	ΔR	0.291	0.167	0.229	
	BE	-1787.42	-1769.40	-1772.69	-1788.17
^{236}Th	**R_{ch}**	5.867	5.788	5.826	
	ΔR	0.299	0.178	0.243	
	BE	-1796.26	-1785.20	-1788.92	-1798.09
^{238}Th	**R_{ch}**	5.884	5.862	5.896	
	ΔR	0.310	0.176	0.245	

Table 2. The Q_α energy in MeV and $T^{\alpha}_{1/2}$ in second for $^{216-238}$Th isotopes obtained from the empirical formulae as in Ref. [41-43] for the NL3 and IOPB-I parameter sets in comparison with experimental data. The $T^{\alpha}_{1/2}$(EXP.) for Viola-Seabrog, Royer and MUDL are determined from Q_α values using experimental BE values.

Nuclei		^{216}Th	^{218}Th	^{220}Th	^{222}Th	^{224}Th	^{226}Th	^{228}Th	^{230}Th	^{232}Th	^{234}Th	^{236}Th	^{238}Th
	NL3	5.195	7.243	7.294	7.092	7.38	6.287	7.355	7.072	5.985	5.684	5.381	5.695
Q_α	IOPB-I	3.588	7.905	7.736	7.415	7.41	6.951	10.524	11.642	11.977	12.502	15.506	6.521
	EXP.	8.073	9.85	8.974	8.131	7.299	6.453	5.521	4.771	4.082	3.671	3.333	3.116
	NL3	9.768	0.294	0.111	0.849	-0.194	4.138	-0.106	0.924	5.540	7.047	8.689	6.989
$T_\alpha^{1/2\,(VS)}$	IOPB-I	22.347	-1.948	-1.403	-0.317	-0.299	1.384	-8.636	-10.776	-11.358	-12.223	-16.295	3.120
	EXP.	-2.473	-7.172	-5.030	-2.650	0.093	3.410	7.913	12.459	17.696	21.510	25.143	27.788
	NL3	10.308	0.676	0.449	1.156	0.059	4.404	0.068	1.071	5.704	7.190	8.814	7.055
$T_\alpha^{1/2\,(R)}$	IOPB-I	23.042	-1.594	-1.083	-2.466	-0.047	1.616	-8.567	-10.773	-11.402	-12.316	-16.477	3.137
	EXP.	-2.083	-6.883	-4.755	-2.386	0.350	3.667	8.186	12.748	18.010	21.822	25.470	28.109
$T_\alpha^{1/2}$ (MUDL)	NL3	14.483	4.749	4.737	5.703	4.819	9.566	5.362	6.681	11.757	13.593	15.581	14.084
	IOPB-I	27.628	2.406	3.155	4.484	4.709	6.688	-3.551	-5.545	-5.901	-6.542	-10.526	10.041
	EXP.	1.692	-3.054	-0.635	2.046	5.120	8.805	13.742	18.735	24.460	28.697	32.774	35.818

Root mean square charge radius

The root mean square (rms) charge radii (R_{ch}) can be used to investigate the deformation in the isotopic chain and can be obtained by adding the finite size of the proton (0.64 fm) using the relation $\sqrt{r_p^2 + 0.64}$. The R_{ch} values for NL3, FSUGarnet, IOPB-I and experimental data [37] are given in Table 1 and their values increase with mass number. The rms neutron-proton radii for ^{220,226,232}Th are calculated at different temperatures using NL3, FSUGarnet and IOPB-I force parameters and shown in the upper panel of Fig. 1 and in the lower panel, the skin thickness is given**.** Here, we noticed that rms radii for all the cases decrease up to the transition temperature (T) and afterwards increases with T. It is minimum for the perfect spherical shape of the nucleus. The values of transition temperature obtained here are also consistent with all other previous calculations i.e the nucleus has a minimum radius at $T=T_c$. The neutron radii for the two forces IOPB-I and NL3 are nearly the same and they overestimate to that the results obtained by FSUGarnet force for all cases. Similar things are also observed in the case of proton radius.

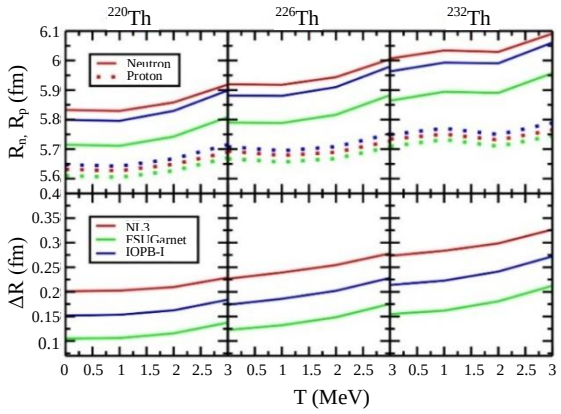

Fig. 1. (Color online) The behavior of rms neutron R_n and proton R_p radii with temperature T for the isotopes ^{220}Th, ^{226}Th, and ^{232}Th with NL3, FSUGarnet and IOPB-I parameter sets are shown. (a) R_n and R_p radii are given in the upper panel and (b) $\Delta R=R_n-R_p$ is in the lower panel respectively.

Neutron-skin thickness

The aggregated number of neutrons on the surface of the nucleus associated with the neutron skin and the skin is decided by the asymmetric arrangement of particles inside the nucleus. The difference between neutron and proton radius is called neutron skin thickness, given as $\Delta R = R_n-R_p$. Our results of ΔR are shown both in Table 1 and the lower panel of Fig. 1 for ^{220,226,232}Th-isotopes. We observed from both the table and figure that ΔR increases monotonically with neutron excess in the isotopic chain of Th for all three parameter sets. We also noticed extended neutron skins in the isotopic chain which reaches 0.31 fm in ^{238}Th nucleus for NL3 and 0.245 fm for IOPB-I sets, respectively. The R_n values cannot be measured with accuracy like R_p due to the neutral nature of neutron. Note that, presently some precise calculations have been done in several laboratories [38,39] and PREX-II experimental data has lots of importance in this regard [40]. The NL3 force parameter has a relatively large asymmetry coefficient as compared to FSUGarnet and thus it gives a greater value of ΔR obtained by the force parameter IOPB-I that is in between the NL3 and FSUGarnet. It can be used in the determination of the EoS and also has an important role in the prediction of neutron star radius.

Nuclear excitation energy

The excitation energy E^* has a lot of importance in the study of the fission process which mainly depends upon the states of the nucleus. It is defined and calculated as $E^*= E(T) – E(T=0)$, where E(T) is the binding energy at a given temperature T and E(T=0) is the binding energy in the ground state. In the upper panel of Fig. 2, the variation of E^* with temperature T for all considered forces is shown for ^{220,226,232}Th as representative cases. It is clear from the figure that the E^* vs. T curve is almost quadratic which agrees with the relation $E^*=aT^2$. It is also observed that E^* for the three forces coincide with each other. A further detailed inspection of the figure shows that the excitation energy suddenly gets blown up after nearly 1 MeV temperature. This signifies the shell melting point, where the shape transition of nuclei takes place.

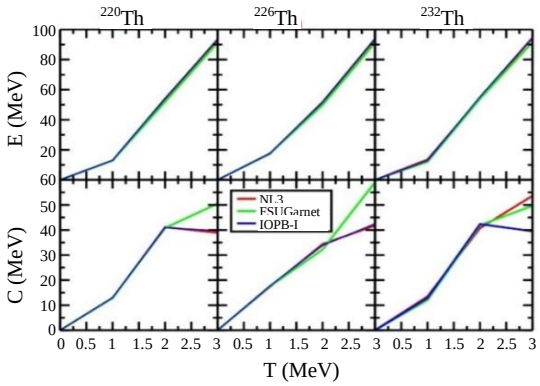

Fig. 2. (Color online) The behaviour of excitation energy E^* and specific heat C(T) with temperature T for the isotopes ^{220}Th, ^{226}Th and ^{232}Th using NL3, FSUGarnet and IOPB-I force parameters are given for comparison in the upper and lower panel respectively.

Specific heat

The specific heats for ^{220,226,232}Th nuclei are calculated to observe the phase transition at critical temperature using the following relation in Eq. (10).

$$\mathrm{C(T)} = \frac{\partial \mathrm{E}^*}{\partial \mathrm{T}} \quad (10)$$

In the lower panel of Fig. 2, the behavior of C(T) is shown. The phenomena as observed for nuclear excitation energy is also reflected in these curves about the critical temperatures i.e 1 MeV where the curve starts a sudden increase. It is observed there are no blows up for ^{226}Th, concluding that this nucleus maintains its spherical shape in all applied temperatures. At low temperatures, all the curves overlap with each other and after the critical value, there are some separations among the curve. It is also noticed that the critical temperature is the same for the above three parameter sets

The Q-value and α-decay half-life

The physics of α-decay is very much crucial for the study of the detailed structures of super-heavy elements. Among all the decay chains, α-decay is the most prominent decay mode for the super-heavy elements. Several formulae have been proposed to study the α-decay half-lives using the decay energy Q_α value, among which three well known phenomenological formulae as given by Viola-Seaborg [41], Royer [42] and modified universal decay law (MUDL) [43] are used for our proposed calculations.

(i) The Viola-Seaborg formula is as follows in Eq. (11).

$$log_{10}T_{\frac{1}{2}}^{\alpha}(VS) = (aZ + b)\frac{1}{\sqrt{Q}} + cZ + d \quad (11)$$

Where the constants a=1.64062, b=-8.54399, c=-0.19430, d -33.9054 are used [41].

(ii) The Royer's formula is given by in Eq. (12).

$$\log_{10} T_{\frac{1}{2}}^{\alpha}(R) = a + bA^{1/6}\sqrt{Z} + \frac{cZ}{\sqrt{Q}} \quad (12)$$

where the constants a=-25.31, b=-1.1629, c=1.5864 the constants are for even(Z)–even(N) nucleus [42].

The improved Royer's empirical formula for α-decay half-lives can be expressed as follows in Eq. (13).

$$\log_{10} T_{\frac{1}{2}}^{\alpha}(mR) = a + bA^{1/6}\sqrt{Z} + \frac{cZ}{\sqrt{Q_\alpha}} + dl(l+1) + h. \quad (13)$$

where the initial three terms are taken from original Royer's formula. The following term contributes centrifugal potential where 'l' represents the angular momentum taken away by the α-particle, and the final 'h' has a role in the blocking effect of an unpaired nucleon and details can be found in Ref. [44].

(iii) The modified universal decay law [43] is formulated as the following in Eq. (14).

$$\log_{10} T_{\frac{1}{2}}^{\alpha}(MUDL) = aZ_dZ_\alpha\sqrt{\frac{A}{Q_\alpha} + b\sqrt{AZ_dZ_\alpha(A_d^{\frac{1}{3}} + A_\alpha^{\frac{1}{3}})}} + c + dI + eI^2 \quad (14)$$

where I= N-Z/A is the asymmetry component.

We have used the original Eq. (12) in our calculations as the logarithmic deviation between the experimental data and theoretical results from the respective Eqs. (12) and (13), and are generally similar for even Z and even N nuclei. The logarithmic half-lives in the isotopic-chain $^{216\text{-}238}$Th using the above empirical formulae are given in Table 2 for the NL3, IOPB-I parameter sets and experimental data. For comparison, we have also given the calculated half-lives using the Q_α values from the experimental binding energies data of Ref. [19,36].

The decay energy (Q_α) is a piece of key information for decay half-life study. It will be used as input for the alpha-decay half-life predictions. The values of Q_α used in the above relations are estimated by using the relation as follows in Eq. (15).

$$Q_\alpha = BE(N,Z) - BE(N-2,Z-2) - BE(2,2) \quad (15)$$

where BE of the α-particle is 28.296 MeV and Z represents the atomic number of parent nuclei. The binding energies of parent (N, Z) and daughter nuclei (N-2, Z-2) are being estimated from the RMF model using NL3 and IOPB-I density functionals. The calculated Q_α values from RMF (NL3 and IOPB-I) are used to estimate the α-decay half-lives for the formulae in Ref. [41-43] are written as $T_{1/2}^{\alpha}$(VS), $T_{1/2}^{\alpha}$ (R), $T_{1/2}^{\alpha}$ (MUDL), respectively.

The Q_α and decay half-lives for the considered isotopic chain using NL3 and IOPB-I sets, and experimental data are given for comparison

which are shown in Table 2 and Fig. 3, respectively. The calculated half-live values using the Q_α results are shown in rows 2 to 4 of Table 2. The $T_{1/2}^{\alpha}$ values are depicted in rows 5 to 13 of the above table. A careful analysis of both Table 2 and Fig. 3 shows a decrease of Q_α with an increase in the mass number and corresponding $T_{1/2}^{\alpha}$ increases linearly with a mass number for the isotopic chain.

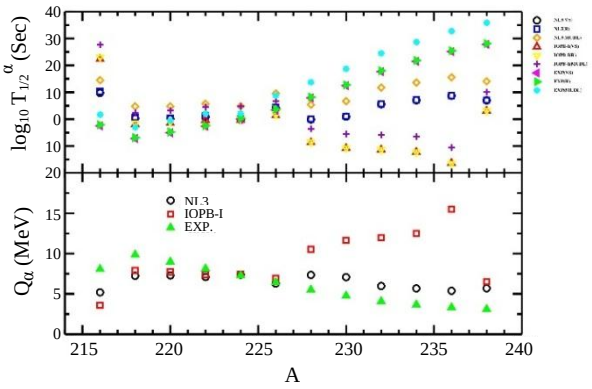

Fig. 3 (Color online) The decay energy Q_α and half-lives $T_{½}^{\alpha}$ for NL3, IOPB-I parameters and experimental data are calculated using Viola-Seaborg, Royer and modified universal decay law formulae which are plotted in lower and upper panels respectively

The Q_α values for RMF (NL3 and IOPB-I) parameters are consistent with the data. The decay energy for Th-isotopes for RMF(NL3) and experimental data decreases with mass number but for the IOPB-I parameter, it decreases up to ^{226}Th then it increases, and a sudden fall for IOPB-I is noticed at ^{238}Th. The Q_α values for ^{226}Th are closer to 6.287, 6.951, and 6.453 MeV respectively for NL3, IOPB-I and the data. In addition to this, for ^{226}Th nucleus, the respective half-live values using Viola-Seaborg, Royer and MUDL formulae are 4.138, 9.566, 8.805 seconds for NL3, 1.384, 1.616, 6.688 seconds for IOPB-I and 3.410, 3.667, 8.805 seconds for the data respectively.

The half-live values using the above three formulae for NL3 and IOPB-I are in order with the experimental data in the considered chain of Th-isotopes. All the results of $T_{1/2}^{\alpha}$ using the above three half-life formulae somehow match with each other. However, among the three half-life formulae used here for the calculation of $T_{1/2}^{\alpha}$, MUDL gives comparatively better results with maximum half-life values for all the considered nuclei in comparison to Viola-Seaborg and Royer formulae. The α-decay energy results for NL3 and IOPB-I differ a little from the data but the decay half-lives show a gross difference in some cases due to the exponential factor. The calculated $T_{1/2}^{\alpha}$ values for different formulae differ from each other for a particular Q_α, which shows a strong correlation between the decay energy and decay half-lives. Among all the formulae used here to calculate the half-live values for this isotopic chain of Th, we are having the maximum and minimum half-live values at ^{216}Th and ^{236}Th respectively. The minimum half-life was observed for the IOPB-I parameter using Viola-Seaborg and Royer formulae. Similarly, the maximum half-life is noted to be using the MUDL formula for the IOPB-I parameter. So, this may be an indication that ^{216}Th and ^{236}Th-isotopes show magicity property.

The β-decay half-life

The β-decay half-life is given empirically by Fiset and Nix [45] to study the stability of the nucleus in Eqs. (16,17).

$$T_\beta = 540 * 10^5 \frac{m_e^5}{\rho_{d.s}(w_\beta^6 - m_e^6)} \quad (16)$$

$$w_\beta = Q_\beta + m_e \quad (17)$$

where w_β is the maximum energy of the emitted β-particle including its rest mass.

The Q_β can be calculated by the following formula [46] in Eq. (18).

$$Q_\beta = BE(Z+1, A) - BE(Z, A) \quad (18)$$

The average density of states of daughter nuclei $\rho_{d.s} = (e^{-A/290}$ *no. of states within 1 MeV of ground state). The β-decay half-lives (T_β) of all the above nuclei are estimated by using the empirical formula given by Fiset and Nix [45] using RMF (NL3) and RMF (IOPB-I) densities. The T_β values are in seconds and hours. Here the Q_β energy and their corresponding β-decay half-lives for N=126-148 of Th-isotopes are calculated for NL3, and IOPB-I parameters as well for the experimental data. We found both negative and positive values of Q_β. It is well known that whenever β-decay energies are greater than zero, then only the β-decay is possible to occur. The negative Q_β value is an indication that β-decay is forbidden, and positive Q_β-values symptomize towards instability region.

The Q_β is found to be negative for $^{216\text{-}234}$Th in case of RMF (NL3) and RMF (IOPB-I) parameter sets and also in case of experimental data where the β-decay is forbidden for the same. The Q_β is positive for the rest two isotopes for both the parameters and data and corresponding T_β values are in tens of seconds. These results are insufficient to analyze the β-stability/instability and further study of above nuclei is needed.

SUMMARY AND CONCLUSIONS

In the present work, we have studied some of the ground state properties for $^{216-238}$Th nuclei. Our results using RMF formalism with NL3, FSUGarnet, and IOPB-I force parameters show an overall agreement with the experimental data. The rms radii for ^{220,226,232}Th at various temperatures are calculated by using NL3 and the other two newly developed FSUGarnet and IOPB-I force parameters. We did not find any substantial difference in the nuclear bulk properties for all the above three sets and also with the experimental data. The positive values of neutron skin thickness indicate extended neutron distribution in comparison to that of proton.

The intrinsic property excitation energy E^* which has a lot of importance in the study of fission process is studied for ^{220,226,232}Th as the representative cases. The E^* suddenly get blow up after nearly 1 MeV temperature signifying the shell melting point, where the shape transition of nuclei take place. Analyzing specific heat variation at different temperature, it is concluded ^{226}Th nucleus maintains its spherical shape with all applied temperatures.

Further, the forces are applied to calculate α-decay half-lives T_α using calculated Q_α-values from RMF (NL3 and IOPB-I) parameter sets, gives satisfactory results. We found that the lowest half-life at ^{236}Th using Viola-Seaborg and Royer formulae for IOPB-I parameter. In addition to this, the maximum half-life is noticed at ^{216}Th using MUDL formula for IOPB-I parameter symbolizes shell closure of its daughter nuclei. The most prominent instability β-decay mode has been analyzed and found that the β-decay is possible for few of nuclei considered here. On studying the decay properties in the isotopic chain for the above series of nuclei we could not find any drastic change, but in brief, more precise study on the finite lifetime of these nuclei may be useful as nuclear fuel for energy production in nuclear reactors.

ACKNOWLEDGMENT

Discussions with Prof. S. K. Patra is greatly acknowledged. This work is partially funded by department of science and technology (DST), Govt. of India Project No. CRG/2019/002691.

AUTHOR CONTRIBUTION

M. Das, K. C. Naik, N. Biswal and R. N. Panda equally contributed as the main contributors of this paper. All authors read and approved the final version of the paper.

REFERENCES

1. W. Nazarewicz, *Nuclear Structure at The Limits*, Proceedings of Eleventh Physics Summer School on Frontiers in Nuclear Physics: From Quark- Gluon Plasma to Supernova, Canberra, Australia (1998) 1.
2. M. Thoennessen, Rep. Prog. Phys. **67** (2004) 1187.
3. P. G. Hansen, Nucl. Phys. **630** (1998) 285.
4. K. Rykaczewski, R. Grzywacz, M. Lewitowicz *et al.*, Nucl. Phys. **630** (1998) 307.
5. L. Satpathy, S. K. Patra and R. K. Choudhury, Pramana J. Phys. **70** (2008) 87.
6. W. M. Howard and P. MÖller, Atom. Data Nucl. Data Tab. **25** (1980) 219.
7. P. Moller, R. J. Nix, W. D. Myers *et al.*, Atom. Data Nucl. Data Tab. **59** (1995) 185.
8. R. N. Panda, M. Bhuyan and S. K. Patra, *Energy Production from Neutron-rich Uranium and Thorium Isotopes*, IEEE International Conference on Engineering Education: Innovative Practices and Future Trends (AICERA) (2012).
9. R. N. Panda, M. Bhuyan and S. K. Patra, Nucl. Phys. At. Energy **70** (2012) 228.
10. A. Quddus, K. C. Naik and S. K. Patra, J. Phys. G: Nucl. Part. Phys. **45** (2018) 075102.
11. A. Quddus, K. C. Naik, R. N. Panda *et al.*, Nucl. Phys. **987** (2019) 222.
12. S. K. Patra, R. K. Choudhury and L. Satpathy, J. Phys. G: Nucl. Part. Phys. **37** (2010) 085103.
13. M. T. S. Kannan, B. Kumar, M. Balasubramanmiam *et al*, Phys. Rev. **95** (2017) 064613.
14. B. Kumar, M. T. S. Kannan, M. Balasubramaniam *et al*., Phys. Rev. **96** (2017) 034623.
15. P. Belli; R. Bernabei; F.A. Danevich *et al.*, Eur. Phys. J. **55** (2019) 140.
16. E. Shin, Y. Lim, C. Ho. Hyun *et al.*, Phys. Rev. **94** (2016) 024320.
17. B. Kumar, S. K. Biswal, S. K. Singh *et al.*, Int. J. Mod. Phys. **25** (2016) 1650020.
18. W. A. Yahya and B. J. Falaye, Nucl Phys. **1015** (2021) 122311.
19. M. Wang, G. Audi, A. H. Wapstra *et al.*, Chin. Phys. **36** (2012) 1603.
20. A. Karim and S. Ahmad, Chin. J. Phys **59** (2019) 606.

21. W.-C. Chen and J. Piekarewicz, Phys. Lett. **748** (2015) 284
22. B. Kumar, B. K. Agrawal and S. K. Patra, Phys. Rev. **97** (2018) 045806.
23. R. J. Furnstahl, B. D. Serot and H. B. Tang, Nucl. Phys. **598** (1996) 539.
24. M. Dutra, O. Lourenco, S. S. Avancini *et al.*, Phys. Rev. **90** (2014) 055203.
25. B. Kumar, S. K. Singh, B. K. Agrawal *et al.*, Nucl. Phys. **966** (2017) 197.
26. J. P. Blaizot, Phys. Rep. **64** (1980) 171.
27. J. Boguta and A. R. Bodmer, Nucl. Phys. **292** (1977) 413.
28. J. I. Fujita and H. Miyazawa, Prog. Theor. Phys. **17** (1957) 360.
29. S. C. Pieper, V. R. Pandharipande, R. B. Wiringa *et al.*, Phys. Rev. **64** (2001) 014001.
30. P. G. Reinhard, M. Rufa, J. Maruhn *et al.*, Z. Phys. **323** (1986) 13.
31. Y. Sugahara and H. Toki, Nucl. Phys. **579** (1994) 557.
32. B. G. Todd-Rutel and J. Piekarewicz, Phys. Rev. Lett. **95** (2005) 122501.
33. C. J. Horowitz and J. Piekarewicz. Phys. Rev. Lett. **86** (2001) 5647.
34. C. J. Horowitz and J. Piekarewicz, Phys. Rev. **64** (2001) 062802.
35. G. A. Lalazissis, J. Koning and P. Ring, Phys. Rev. **55** (1997) 540.
36. Anonymous, National Nuclear Data Center, Brookhaven National Laboratory. https://www.nndc.bnl.gov/. Retrieved in January (2021).
37. I. Angeli, K. P. Morinova, Atom. Data Nucl. Data Tab. **99** (2013) 69.
38. A. Trzcinska, J. Jastrzebski, P. Lubinski *et al.*, Int. J. Mod. Phy. **87** (2001) 082501.
39. J. Jastrzebski, A. Trzcinska, P. Lubinski *et al.*, Int. Mod. Phys. **13** (2004) 343.
40. S. Abrahmyan, Z. Ahmed, H. Albataineh *et al.*, Phys. Lett. **108** (2012) 112502.
41. V. E. Viola and G. T. Seaborg, J. Inorg, Nucl. Chem. **28** (1966) 741.
42. G. Royer and H. F. Zhang, Phys. Rev. **77** (2008) 037602.
43. D. T. Akrawy, H. Hassanabadi, S. S. Hossein *et al.*, Int. J. Mod. Phys. **28** (2019) 1950075.
44. J. G. Deng, H. F. Zhang and G. Royer, Phys. Rev. **101** (2020) 034307.
45. E. O. Fiset and J. R. Nix, Nucl. Phys. **193** (1972) 647.
46. B. Kumar, S. K. Biswal, S. K. Singh *et al.*, Phys. Rev. **92** (2015) 054314